Eddy Diffusivity for Distillation Sieve Trays

Douglas L. Bennett and Henry J. Grimm
Air Products and Chemicals, Inc., Allentown, PA 18195

An understanding of the eddy diffusivity on a distillation tray is important to accurately predict the distillation tray efficiency from the point efficiency. This article presents a new correlation to predict liquid-phase eddy diffusivity (De) on sieve trays. This correlation has been developed by modeling backmixing as the trajectory motion of liquid droplet elements through the two-phase layer height on the tray. The trajectory model indicates that De is a strong function of the two-phase layer height. An expression for froth height is derived.

The new De correlation offers two main improvements over existing literature correlations. First, this model is phenomenologically-based and, therefore, not limited to air/water. Second, the new De correlation gives significantly lower average actual and relative errors and a lower standard deviation of the actual error than do other available correlations.

Introduction

The Murphree tray efficiency of a distillation tray can be substantially higher than the local point efficiency. This improvement in Murphree efficiency results from the crossflow staging effect that occurs on industrial-scale distillation trays.

Requirements for the accurate design of high-efficiency large-diameter distillation trays have resulted in the development and application of detailed numerical models (Fox et al., 1986), which simulate the behavior of the distillation column. Inputs to such programs include inlet velocity profiles, the local point efficiency, the geometry of the tray, and the characteristics of the eddy diffusivity. Such models can also account for the impact of vapor mixing, entrainment and weeping.

The results of these models can provide, over a wider operating range, more accurate predictions of performance than are possible with simpler, one-dimensional models. In addition, such models can be used to optimize tray designs and shorten the time to develop these concepts.

The accuracy of both simple and more complex models depends on the accuracy of the correlations to describe the fundamental phenomena occurring on the tray. The relevant hydraulic phenomena are: convective flow patterns, entrainment, weeping, vapor mixing, and the eddy diffusivity of the froth. For typical operating conditions and tray designs, the eddy diffusivity of the froth can be the most important of these phenomena.

Correspondence concerning this article should be addressed to D. L. Bennett.

Liquid backmixing on rectangular sieve trays has been examined in several air/water studies. These works include Barker and Self (1962), Gilbert (1959), Foss (1957), Shore and Haselden (1969), Porter et al. (1977), and Raper et al. (1984). In these experiments, dye or salt tracers were introduced close to the inlet or outlet weir, and the upstream (or downstream) tracer concentration profile was measured. The extent to which a tracer is able to migrate upstream is a measure of backmixing. Either eddy diffusivity (*De*) or Peclet number (*Pe*) was back-calculated using the concentration data and steady-state or unsteady-state material balances on the tray. Determination of *De* in these studies is based on the assumption that liquid backmixing is isotropic and is superimposed on a bulk liquid flow. In general, the concept of eddy diffusivity should be applied only for uniform random eddies and thus cannot be invoked to characterize localized circulation patterns, which can be caused, for example, by the influence of wall curvature. Since the air/water tests described in the above references were all conducted on rectangular trays, nonrandom mixing effects were minimal. Therefore, the eddy diffusion theory should apply for these conditions.

Table 1 shows the ranges of the hydraulic and operating parameters used in the literature tests. Table 1 indicates that 86 total data points were obtained from the group of researchers, 63 of which were taken by Barker and Self (1962). These data were used to develop a composite database for *De*.

Barker and Self's work encompassed a broad range of liquid and vapor rates and weir heights. Their experiments included

Table 1. Operating and Hydraulic Parameters for Rectangular Sieve Tray Air/Water Liquid Backmixing Studies

Authors	No. of Data Points	h_w m	D_H m	A_H/A_T	L_T m	K_s m/s	$\dot{Q}_L$ 10^{-3}m^3/s·m Weir
Barker & Self	63	0.0254–0.1020	0.00476	0.06	0.826–1.4	0.0152–0.0792	1.04–10.4
Gilbert	6	0.0254–0.0508	0.00476	0.06	0.775	0.0183–0.0396	2.16–4.3
Foss	8	0.0254–0.0965	0.00476	0.106	0.914	0.0213–0.0640	2.36–25.58
Porter et al.	9	0.0254	0.01270	0.07	1.650	0.0299–0.0790	1.42

results from both steady-state and unsteady-state liquid mixing tests. The steady-state tests were conducted by continuous injection of the tracer close to the outlet weir onto a tray having constant liquid and vapor loadings.

A steady-state material balance yields the following differential equation:

$$\frac{1}{Pe}\frac{d^2x}{dz^2}-\frac{dx}{dz}=0 \tag{1}$$

where
x = tracer mole fraction
z = fractional distance along liquid path length

Solution of Eq. 1 yields:

$$\frac{x-x_o}{x_g-x_o}=\frac{\exp[Pe\ z]-1}{\exp[Pe]-1} \tag{2}$$

where
x = tracer mole fraction at any point z
x_g = tracer mole fraction at the injector
x_o = tracer mole fraction entering tray

Since x, x_o, and x_g, and z were measured in these tests, Pe could be backcalculated using Eq. 1. Finally, De was determined from the Peclet number (Pe):

$$De=\frac{UL_T}{Pe} \tag{3}$$

where
U = superficial liquid velocity
L_T = liquid path length

Since the trays used in these tests were rectangular, determination of U and L_T is fairly straightforward. For our current analysis, the literature values for Pe were utilized. However, U was computed using h_L calculated by the methods developed by Bennett et al. (1983), Eq. 17.

Barker and Self (1962) also determined De from unsteady-state tracer tests, in which a fixed volume of water was charged to the tray with constant vapor flow and a fixed amount of dye added at the tray centerline. This tray was referred to as a "static" tray since there was no net liquid flow across the tray. Dye concentration was measured over time at various locations to yield unsteady-state concentration profiles. De was then directly backcalculated from the solution of the unsteady-state concentration profile. Since the static tray tests did not include liquid rates, weir heights, etc., those De data were not included in the 86 data point subset used in the present study to develop a new De correlation. However, predictions from the De correlation derived by Barker and Self from their static tray were compared to the experimental results.

Gilbert (1959) obtained Pe data for both bubble cap and sieve trays. Only his sieve tray results are considered here. Gilbert used an unsteady-state diffusion model and frequency response data to backcalculate Pe from the transfer function of exit concentration with respect to the inlet concentration. De was calculated for the present analysis using Eq. 3.

Shore and Haselden (1969) used Foss's (1957) residence time distribution data on sieve trays to determine eddy diffusivity. Foss conducted unsteady-state air/water tracer tests, in which a step change was applied to the inlet salt (tracer) concentration and the downstream concentration measured over time. Shore and Haselden analyzed Foss's data by considering the case of a pulse of salt tracer injected into the center row of holes of a sieve tray on which there is no net liquid flow. After a short time span, the tracer distribution would be sharply peaked. Over time, the spread would increase symmetrically, eventually becoming uniform along the tray. The distance variance, σ^2, would increase linearly with time, where

$$\sigma^2=2\ De\ t \tag{4}$$

Details of the analysis leading to Eq. 4 are included in Shore and Haselden (1969). From plots of σ^2 vs. t, Shore and Haselden determined De, noting that De is essentially independent of liquid rate. From that observation, they hypothesized that when a net flow of liquid on the tray is superimposed on the bubbling action, the momentum is transmitted uniformly through the foam and the distance distribution is moved downstream intact. Shore and Haselden concluded that the momentum of the eddies is derived from the energy of the rising vapor, and thus eddy size is mainly a function of foam height.

Porter et al. (1977) used the apparatus and steady-state analysis method of Barker and Self (1962) to determine the extent of backmixing for the spray regime. They identified the froth-to-spray transition as being characterized by a rapid increase in eddy diffusivity with increasing vapor rate. Their nine data points (four "froth" and five "spray" points), indicated in Table 1, were incorporated into the De database used in the present analysis.

A more recent investigation by Raper et al. (1984) examined liquid mixing only for trays operating in the spray regime and concluded that De decreased as the flow on the tray passed from the froth-to-spray transition. Once in the spray regime, Raper et al. reported that De continues to decrease as the vapor rate increases. These results contradict those of Porter et al., in part because Raper et al. used an analysis (unsteady-state RTD curves) which they claim is more valid for calculating De

in the spray regime. Since the present analysis is concerned mainly with the froth regime and the results of Raper et al. are not fully understood, Raper's data is not included in the literature database examined here.

Development of a New *De* Correlation

Previous De correlations

Several eddy diffusivity correlations have been presented including: *Bubble Tray Design Manual* (1958), Barker and Self (1962), Foss and Gerster (1958), and Shore and Haselden (1969). Each of these correlations was obtained by regressing some of the air/water liquid mixing data on rectangular sieve trays described in the previous section. All available *De* correlations (*De* in units of m^2/s) are:

Bubble Tray Design Manual (1958):

$$De = [0.0124 + 0.0558\ V_s + 12.078\ \dot{Q}_L + 0.5906\ h_w]^2/10.764 \quad (5)$$

where

V_s = superficial vapor velocity, m/s
h_w = outlet weir height, m

Barker and Self (1962)—Static Tray (No Net Liquid Flow):

$$De = 0.006673\ V_s^{1.44} + 0.09216\ h_L - 0.00562 \quad (6)$$

where

h_L = clear liquid holdup on tray, m
V_s = superficial vapor velocity, m/s

Foss and Gerster (1958):

Barker and Self fitted their data to a correlation method suggested by Foss and Gerster and obtained the following:

for $h_w = 0.0254$ m (1.0 in.)

$$De = 3.745 \times 10^{-4} h_L^{-2.02} u^{0.02} h_{2\phi}^{3.02} \quad (7a)$$

for $h_w > 0.0254$ m

$$De = 0.00166 h_L^{-1.91} u^{0.09} h_{2\phi}^{2.91} \quad (7b)$$

Shore and Haselden (1969):

$$De = 0.3093 h_{2\phi} K_s^{0.63} \quad (8)$$

To allow comparison of the equations on a consistent basis, a common correlation for $h_{2\phi}$ is needed. For this investigation, $h_{2\phi}$ is calculated from Eq. 26. In addition, h_L is calculated using Eq. 17a.

Table 2 lists the actual and relative errors for these correlations. Definitions of the errors computed are given in Table 2. All previous correlations except for the correlation in the *Bubble Tray Design Manual* overpredict *De*, as indicated by an average relative error that is less than zero. Of the group, this equation gives the smallest average absolute relative error. As seen in Figure 1 for conditions with high outlet weirs, this method is fairly accurate, but large errors result at low weir height.

The overall high error level of these four correlations may be due in part to the use of our proposed correlations for h_L

Table 2. Relative and Actual Errors for Eddy Diffusivity Correlations

Authors	Avg. Actual Error m^2/s	Avg. Abs. Actual Error m^2/s	Std. Dev. Actual Residual m^2/s	Avg. Rel. Error %	Avg. Abs. Rel. Error %
De Correlation					
Bubble Tray Design Manual	0.0023	0.0034	0.0045	31.0	40.7
Barker & Self	−0.0028	0.0034	0.0029	−67.6	83.2
Foss & Gerster	−0.0061	0.009	0.0197	−14.9	106.3
Shore & Haselden	−0.0021	0.0026	0.0025	−47.0	58.8
Proposed Trajectory Model	0.0005	0.0013	0.0020	5.9	24.0

Relative Error

$$\%\ \text{Rel. Error}_i = \left(\frac{De\ \text{Data} - De\ \text{calc.}}{De\ \text{Data}}\right)_i \times 100$$

$$\%\ \text{Avg. Rel. Error} = \frac{\sum_{i=1}^{N} \text{Rel. Error}_i}{N}$$

where N = total number of points

$$\%\ \text{Avg. Abs. Rel. Error} = \frac{\sum_{i=1}^{N} |\text{Rel. Error}_i|}{N}$$

Actual Error

$$\text{Actual Error}_i = (De\ \text{Data} - De\ \text{Calc.})_i$$

$$\text{Avg. Actual Error} = \frac{\sum_{i=1}^{N} \text{Actual Error}_i}{N}$$

$$\text{Avg. Abs. Actual Error} = \frac{\sum_{i=1}^{N} |\text{Actual Error}_i|}{N}$$

$$\text{Std. Dev. of Actual Residual} = \left[\frac{\sum_{i=1}^{N} (De\ \text{Data} - De\ \text{Calc.})_i^2}{N-1}\right]^{0.5}$$

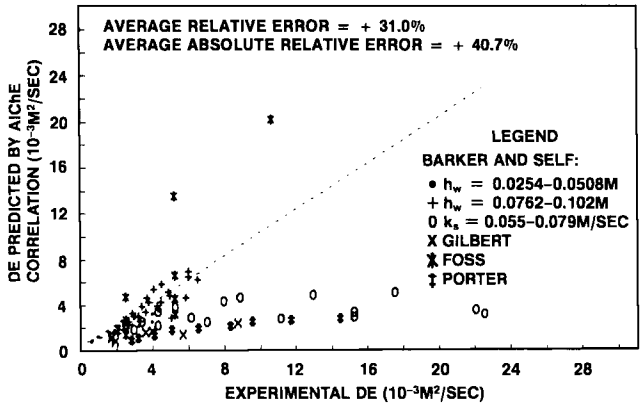

Figure 1. Correlation for *De*: *Bubble Tray Design Manual* vs. the data.

and $h_{2\phi}$, rather than using the methods used to calculate these parameters by the authors. Our proposed correlations have been substituted for two main reasons: 1) to provide a consistent basis for comparison, i.e., to deal with one h_L correlation, rather than four methods to estimate h_L; and 2) to use the most accurate correlations available. In particular, it was assumed that the use of predicted values of h_L would be better than using h_L values based on floor-mounted manometer data, which Bennett et al. (1983) have shown to be generally in error.

Trajectory model for eddy diffusivity

No existing eddy diffusion correlation is successful in predicting the available *De* data. The *De* correlations described above have the basic shortcoming that no physical or mechanistic backmixing model was used to develop a mechanistic correlation.

Our eddy diffusivity model assumes the following factors:

- The theory of eddy diffusion applies: the backmixing is uniform and random.
- There are at least two possible mechanisms for backmixing on a sieve tray: diffusion results from 1. turbulence in the liquid continuous region and 2. motion of liquid droplets in the vapor continuous region. This model assumes that the principal mechanism is the droplet motion mechanism.
- The fluid and vapor exist typically in a liquid continuous region near the tray and a vapor continuous region farther away from the tray surface. It is quite complicated, however, to consider separate mixing mechanisms in the liquid and vapor continuous regions. To develop a simple relationship and to approximately account for eddy diffusion in the liquid continuous region, droplet mass exchange is assumed to occur over the entire two-phase layer height, $h_{2\phi}$.

Figure 2 shows the backmixing trajectory model, which interchanges the flow between cells i and $i+1$ and the forward and backward flow paths of liquid droplets having trajectory angle θ. The main goal of the following analysis is to derive expressions for θ and *De*. Since this derivation is based on a basic ballistic calculation method, the details are not given here.

The trajectory range for the liquid droplets is:

$$\delta = \frac{2v_x^2 \tan\theta}{g} \tag{9}$$

An expression for v_x is obtained by using the relationship between v_x and the maximum height attained by the droplets, $h_{2\phi}$.

$$v_x = \left[\frac{2gh_{2\phi}}{\tan^2\theta}\right]^{1/2} \tag{10}$$

An expression for δ is obtained by substituting Eq. 10 into Eq. 9:

$$\delta = \frac{4h_{2\phi}}{\tan\theta} \tag{11}$$

If we use Fick's law as the defining equation for eddy diffu-

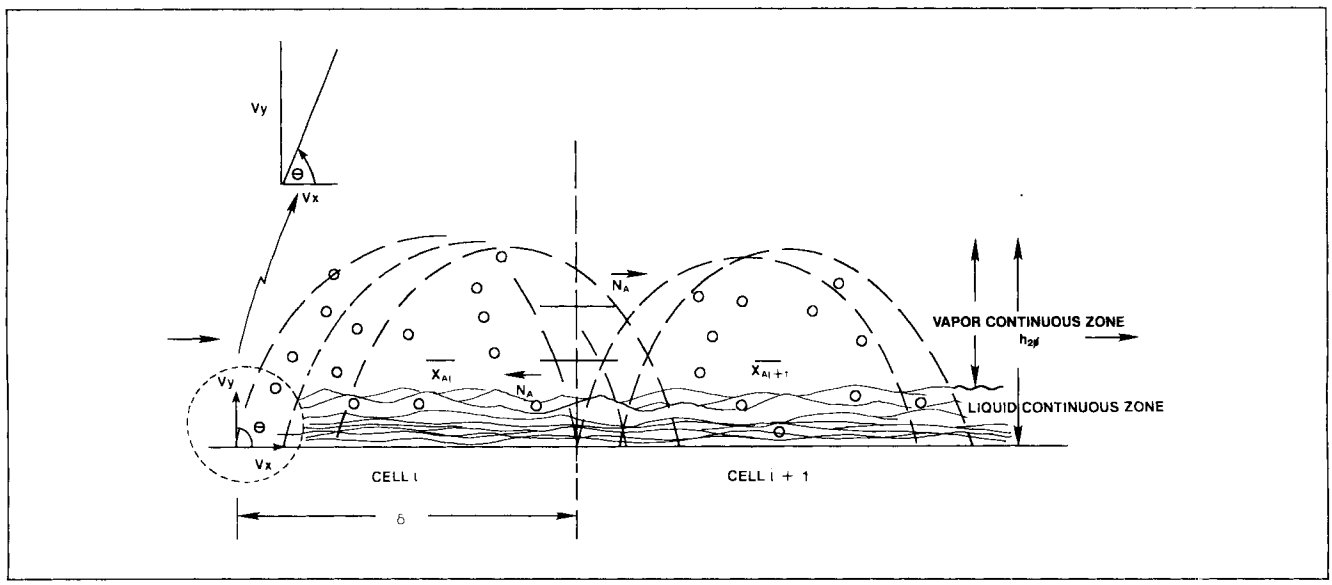

Figure 2. Liquid backmixing trajectory model.

sivity, the net molar flow of species A in turbulent flow is given by (assuming constant molar bulk density ρ):

$$N_A = -h_{2\phi}\phi_{2\phi}De\rho\frac{(x_{A_{i+1}}-x_{A_i})}{\delta} \tag{12}$$

where

$x_{A_{i+1}}$ = average liquid mole fraction of component A in cell $i+1$

$\phi_{2\phi}$ = relative two-phase layer density = $\rho_{2\phi}/\rho_L$, where $\rho_{2\phi}$ is the two-phase layer density; product of $h_{2\phi}\phi_{2\phi}$ = clear liquid holdup (h_L) = liquid flow cross-sectional area per unit weir length

The net flow is the difference between the forward and backward flows crossing the boundary between cells i and $i+1$

$$N_A = \vec{N}_A - \overleftarrow{N}_A = v_x h_{2\phi}\phi_{2\phi}\rho(x_{A_i}-x_{A_{i+1}}) \tag{13}$$

Equating Eqs. 12 and 13 yields:

$$v_x = \frac{De}{\delta} \tag{14}$$

v_x is eliminated from Eq. 14 by substituting Eq. 10:

$$\frac{(2g\ h_{2\phi})^{1/2}}{\tan\theta} = \frac{De}{\delta}$$

δ is then eliminated by substituting Eq. 11, and rearranging it gives the following:

$$\frac{De}{(2h_{2\phi}^3 g)^{1/2}} = \frac{4}{\tan^2\theta} \tag{15}$$

Equation 15 demonstrates that if the assumed mechanism is valid, the appropriate dimensionless grouping is a Froude number, $v_x^2/gh_{2\phi}$ or $De^2/gh_{2\phi}^3$. This grouping is a function of the trajectory angle θ, which may depend on the flow conditions. Solving for the eddy diffusivity,

$$De = \frac{4[2h_{2\phi}^3 g]^{1/2}}{\tan^2\theta} \tag{16}$$

The above equation allows the determination of De if $h_{2\phi}$ and θ are known.

Model development for $h_{2\phi}$

The Bennett et al. correlation for the liquid inventory portion of the tray pressure drop is:

$$h_L = \phi_e[h_{Fe}] \tag{17a}$$

where

$$h_{Fe} = h_w + C\left(\frac{\dot{Q}_L}{\phi_e}\right)^{2/3} \tag{17b}$$

and

$$\phi_e = \exp[-12.55K_s(\text{m/s})^{0.91}] \tag{17c}$$

$$C = 0.501 + 0.439\exp[-137.8h_w(\text{m})] \tag{17d}$$

where h_{Fe} is the effective height of the liquid continuous portion of the froth. During the development of this correlation, h_{Fe} was *not* based on observed froth height measurements, but was derived from the total tray pressure drop data taken from many literature sources.

In this model, the total froth height $h_{2\phi}$ is assumed to consist of a liquid continuous region, which is characterized (not equal, since h_{Fe} is a derived hydraulic thickness, assuming uniform froth density) by h_{Fe} and a spray region formed by droplets ejected from the top of the effective froth height h_{Fe}.

The height of the ejected droplet may be influenced by the drag on the droplet and gravity. The governing equation is:

$$M_D\frac{dV_D(t)}{dt} = -M_D g - F_D(t). \tag{18}$$

Using the definition of the drag coefficient to estimate $F_D(t)$:

$$F_D(t) = \frac{\pi D^2}{4}\Delta P_D(t) = \frac{\pi D^2}{4}\frac{k_D\rho_V[V_D(t)-V_s]^2}{2}. \tag{19}$$

Therefore, the differential equation for the droplet velocity becomes:

$$\frac{dV_D(t)}{dt} = -g \pm \frac{3}{4}\frac{k_D}{D}\frac{\rho_V}{\rho_L}[V_D(t)-V_s]^2 \tag{20}$$

where the negative sign is used for $V_D(t) > V_s$ and the positive sign for $V_D(t) < V_s$.

Using the definition of K_s, and $\rho_V << \rho_L$,

$$\frac{dV_D(t)}{d_t} = -g \pm \frac{3}{4}\frac{k_D}{D}\left(\frac{V_D(t)}{V_s}-1\right)^2 K_s^2 \tag{21}$$

The influence of the drag force on the throw height of the droplet will depend on V_D/V_s, K_s and the droplet size D. For droplet sizes larger than 1 mm, the second term is usually less than about 10% of g. Therefore, the second term will be neglected and the solution yields:

$$h_{2\phi} = h_{Fe} + \frac{V_{Do}^2}{2g} \tag{22}$$

where V_{Do} is the initial ejection velocity from the effective froth layer of height h_{Fe}.

To determine $h_{2\phi}$, V_{Do} must be estimated. As the vapor leaves the tray perforation, it will decelerate rapidly from a velocity of V_H to a velocity of about $V_s/(1-\phi_e)$. It will be assumed that this vapor momentum loss will be accomplished by momentum exchange with the liquid near the bottom of the tray. It is also assumed that the liquid momentum of the liquid returning to the tray floor will be consumed by liquid impact against the tray floor with an average velocity of $\bar{V}_L$. Equating the momentum loss of the vapor to impact momentum loss of the liquid gives,

$$(\rho_V V_s A_T)\left(V_H - \frac{V_s}{1-\phi_e}\right) = \rho_L A_{L_D} \overline{V}_L^2 \qquad (23)$$

where A_{LD} is the area of downward liquid flow, and $\overline{V}_L$ is the average downward liquid velocity.

If it is assumed that the eddy viscosity is constant, the liquid velocity profile entering the region, where momentum exchange occurs, can be assumed to be parabolic. As derived in the Appendix, A_{LD} can be estimated as $A_L/(3)^{0.5}$, since $A_L = \phi_e A_T$, $A_{LD} = \phi_e A_T/(3)^{0.5}$. Therefore, assuming $V_s/(1-\phi_e)$ is much less than V_H and $\rho_V << \rho_L$, solving for $\overline{V}_L$ gives,

$$\overline{V}_L = \left[\frac{(3)^{0.5}}{(A_H/A_T)\phi_e}\right]^{1/2} K_s \qquad (24)$$

Because of the parabolic velocity profile, the maximum upward velocity, $V_{\max}$ can be evaluated in terms of $\overline{V}_L$. In the Appendix, the relationship $V_{\max} = 3\overline{V}_L$ is derived. Therefore,

$$V_{\max} = 3\left[\frac{(3)^{0.5}}{(A_H/A_T)\phi_e}\right]^{1/2} K_s \qquad (25)$$

whether the liquid ejection velocity V_{Do} increases or decreases depends on further momentum exchange between vapor and liquid, viscous dissipation, and other losses. But, for now, it will be assumed that $V_{Do} = V_{\max}$. Combining Eqs. 22 and 25 gives,

$$h_{2\phi}(\mathrm{m}) = h_{Fe}(\mathrm{m}) + 0.794\frac{K_s^2}{(A_H/A_T)\phi_e} \qquad (26)$$

Measurements of $h_{2\phi}$ are highly subjective, especially for the air/water system. Subsequent work has compared the values of Eq. 26 against froth heights determined from entrainment rates, and Eq. 26 appears reasonable. Because of the phenomenological basis, Eq. 26 will be used in the correlation for *De*. Equation 26 should capture the primary mechanics governing the froth height.

Evaluation of the trajectory angle, θ

At this point the trajectory angle, θ, is unknown. If θ is assumed to be constant, then the lefthand side of Eq. 15 is also a constant: that is, θ could be calculated by using Eq. 15 to regress the *De* data. A plot of $De/(2h_{2\phi}^3 g)^{1/2}$ vs. F_s was made in Figure 3a to check if θ is approximately constant. F_s was chosen as the independent variable in Figure 3a because it was suspected that θ might be a function of the hole velocity. Based on single-phase turbulent jet data, however, θ would be expected to be constant at about 80°: that is, the edge of the jet would be about 10° measured from the vertical. Figure 3a suggests no significant dependency of θ on F_s for the range of F_s included in the literature database. With the exception of several of Porter's points, most of data is clustered around a y-axis value (lefthand side of Eq. 15) of about 0.02, which corresponds to a value of θ equal to 86° or 4° from the vertical. A plot of the Peclet number, $De/(2h_{2\phi}^3 g)^{1/2}$, vs. Froude number using K_s instead of F_s also does not indicate any functionality. Figure 3b plots $De/(2h_{2\phi}^3 g)^{1/2}$ vs. a Froude number, $F_s^2/(gD_H)$. As the Froude number increases, the Peclet number then decreases slightly. This may result from some partial shifting from a froth regime to a jetting regime. However, little error is introduced by assuming that $De/(2h_{2\phi}^3 g)^{1/2}$ is constant for all the values of F_s^2/gD_H.

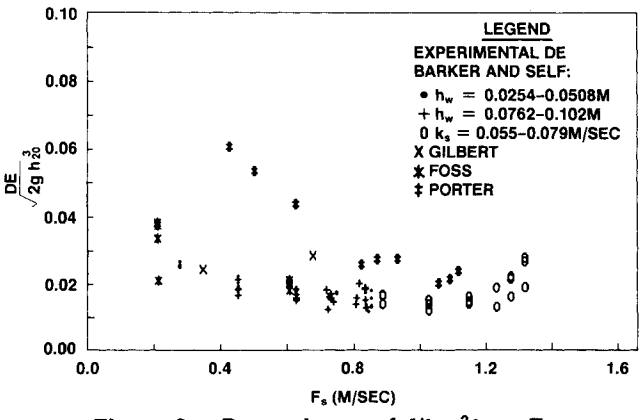

Figure 3a. Dependency of $4/\tan^2\theta$ on F_s.

Conclusions and Summary

Available sources of eddy diffusivity data have been accumulated into a common database. This database included 86 sets of data from four literature sources.

A mechanistic model was developed which was based on the assumption that backmixing occurs by the physical transport of droplet elements. This analysis shows that the two-phase froth height ($h_{2\phi}$) and the effective trajectory angle θ are important. Based on a regression of the available data, the relationship for eddy diffusivity is,

$$De(\mathrm{m}^2/\mathrm{s}) = 0.02366[h_{2\phi}(\mathrm{m})]^{3/2}[g(\mathrm{m/s}^2)]^{1/2} \qquad (27a)$$

or

$$\frac{De}{(gh_{2\phi}^3)^{1/2}} = 0.02366 \qquad (27b)$$

where

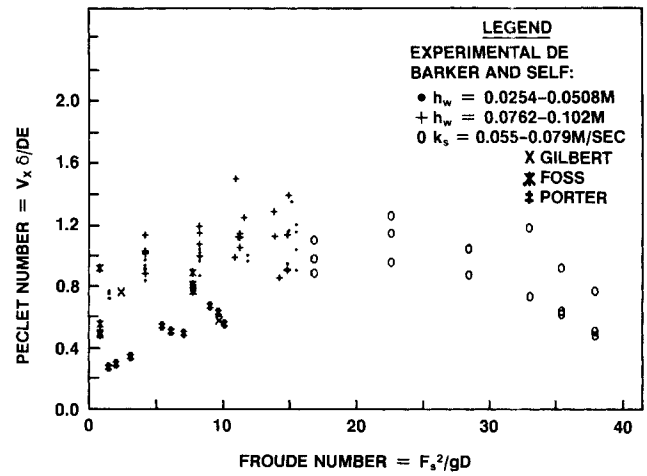

Figure 3b. Dependency of Peclet number on Froude number.

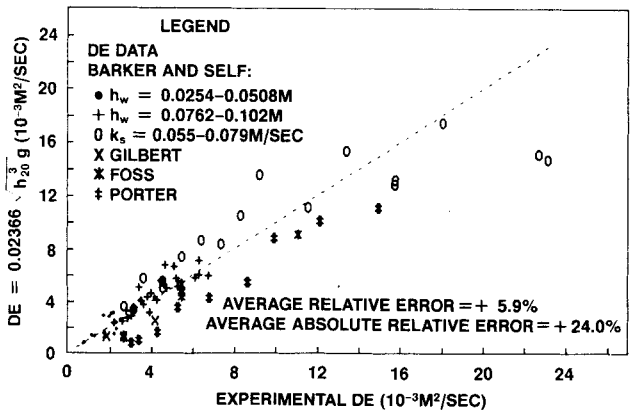

Figure 4. Calculated *De* (Eq. 27) vs. the data.

$$h_{2\phi}(\mathrm{m}) = h_{Fe}(\mathrm{m}) + \left[\frac{0.794[K_s(\mathrm{m/s})]^2}{(A_H/A_T)\phi_e}\right] \tag{26}$$

$$h_{Fe}(\mathrm{m}) = C\left[\frac{\dot{Q}_L[\mathrm{m^3/(m\cdot s)}]}{\phi_e}\right]^{2/3} + h_w \tag{17b}$$

$$\phi_e = \exp[-12.55K_s(\mathrm{m/s})^{0.91}] \tag{17c}$$

$$C = 0.501 + 0.439\exp[-137.8h_w(\mathrm{m})] \tag{17d}$$

To test the predicted functionality, a power fit regression based on the residual between the experimental and calculated *De* values (i.e., the actual error) yielded 1.57 for the exponent on $h_{2\phi}$. This result supports the model and Eq. 27.

Equation 27 gives an average relative error of 5.9% and an average absolute relative error of 24%. This is a substantial improvement over previously available correlations, as observed in Table 2. The average actual error in *De* is also much lower for the proposed correlation, 5.0×10^{-4}m²/s as compared to a range of -0.0021 to $+0.0023$ m²/s for the other correlations. The standard deviation of the actual error was computed for each correlation, showing that the proposed model has the relatively low value of 0.002 m²/s compared to the 0.0025–0.0197 m²/s range for the literature correlations.

In Figure 4, a parity plot is given to allow a comparison of the calculated *De* values from Eq. 27 to the data. As indicated in Eq. 27, *De* is expected to be a unique function of the froth height, $h_{2\phi}$. In Figure 5, *De* is plotted directly against $h_{2\phi}$, where $h_{2\phi}$ is calculated from Eq. 26. The solid line indicates the best third-order polynominal fit, the dashed line indicates values given from Eq. 27. Based on the scatter that exists, both curve fits are equivalent if $h_{2\phi}$ exceeds 0.1 m (4 in.). For conditions yielding $h_{2\phi}$ less than 0.1 m, the data support a minimum value for *De* of about 0.0023 m²/s.

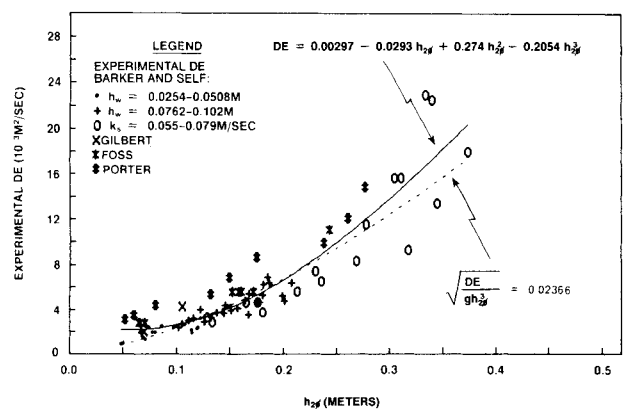

Figure 5. Experimental *De* vs. $h_{2\phi}$ (Eq. 22).

Notation

A_H/A_T = fractional open area on tray
C = constant defined in Eq. 17d
ΔC = incremental change in liquid concentration, kmol/m³
D = liquid droplet diameter, m
De = liquid-phase eddy diffusivity, m²/s
$F_D(t)$ = drag force acting on a liquid droplet, N
F_s = density corrected vapor hole velocity $= V_H[\rho_V/(\rho_L-\rho_V)]^{1/2}$, m/s
h_{Fe} = effective froth height, m
h_L = clear liquid holdup on tray, m
h_w = outlet weir height, m
$h_{2\phi}$ = two-phase layer height on tray (sum of liquid continuous region + vapor continuous region), m
k_D = head loss coefficient relating $F_D(t)$ to velocity
K_s = density corrected superficial vapor velocity over bubbling tray area $= V_s[\rho_V/(\rho_L-\rho_V)]^{1/2}$, m/s
L_T = liquid path length on tray, m
M_D = mass of a liquid droplet, kg
N_A = net molar flow rate of species A, kmol/s·m
Pe = Peclet number, UL_T/De
$\dot{Q}_L$ = flow rate of liquid per unit weir length (liquid loading), m³/m weir·s
U = superficial liquid velocity on tray, m/s
$V_D(t)$ = velocity of a liquid droplet, m/s
v_x = x-component of trajectory velocity, m/s
v_y = y-component of initial trajectory velocity, m/s
V_H = vapor velocity through holes on sieve tray based on A_H, m/s
V_s = superficial vapor velocity on bubbling surface of tray, m/s
x_{Ai} = average liquid-phase mole fraction of species A in cell i
x_{Ai+1} = average liquid-phase mole fraction of species A in cell $i+1$
x_g = tracer mole fraction at injector
x_o = tracer mole fraction entering tray
z = fractional distance along liquid path length

Greek letters

δ = range of trajectory, m
$\Delta P_D(t)$ = drag pressure acting on a liquid droplet, N/m²
θ = trajectory angle, deg
ρ = liquid molar density, kmol/m³
ρ_f = froth density, kg/m³
ρ_L = liquid mass density, kg/m³
ρ_V = vapor mass density, kg/m³
$\rho_{2\phi}$ = two-phase layer density, kg/m³
σ^2 = distance variance, Eq. 4, m²
ϕ_e = effective relative froth density as defined by Bennett et al. (1983)
$\phi_{2\phi}$ = overall relative two-phase density $= \rho_{2\phi}/\rho_L = \phi_e h_{Fe}/h_{2\phi} = h_L/h_{2\phi}$

Literature Cited

Barker, P. E., and M. F. Self, "The Evaluation of Liquid Mixing Effects on a Sieve Plate Using Unsteady and Steady-State Tracer Techniques," *Chem. Eng. Sci.*, **17**, 541 (1962).

Bennett, D. L., R. Agrawal, and P. J. Cook, "New Pressure Drop Correlation for Sieve Tray Distillation Columns," *AIChE J.*, **29**(3), 434 (1983).

Bubble Tray Design Manual, AIChE, New York (1958).

Foss, A. S., "Liquid Mixing on Bubble Trays and Its Effect Upon Plate Efficiency," PhD Thesis, Univ. of Delaware (1957).
Foss, A. S., J. A. Gerster, and R. L. Pigford, "Effect of Liquid Mixing on the Performance of Bubble Trays," *AIChE J.*, **4**(2), 231 (1958).
Fox, V. G., R. M. Thorogood, and D. H. S. Ying, "Performance Prediction for a Maldistributed Tray Distillation Column Using a Multicell Model with Intercell Mixing Flows," AIChE Nat. Meeting, Miami Beach, FL (Nov., 1986).
Gilbert, T. J., "Liquid Mixing on Bubble Cap and Sieve Plates," *Chem. Eng. Sci.*, **10**, 243 (1959).
Porter, K. E., S. Safekourdi, and M. J. Lockett, "Plate Efficiency in the Spray Regime," *Trans. Inst. Chem. Engrs.*, **55**, 190 (1977).
Raper, J. A., W. V. Pinczewskii, and C. J. D. Fell, "Liquid Passage on Sieve Trays Operating in the Spray Regime," *Chem. Eng. Res. Des.*, **62**, 111 (Mar. 1984).
Shore, D., PhD Thesis, Univ. of Leeds, England (1968).
Shore, D., and G. G. Haselden, "Liquid Mixing on Distillation Plates and Its Effect on Plate Efficiency," *Inst. Chem. Engrs. Symp. Ser.*, No. 32, 2:54 (1969).

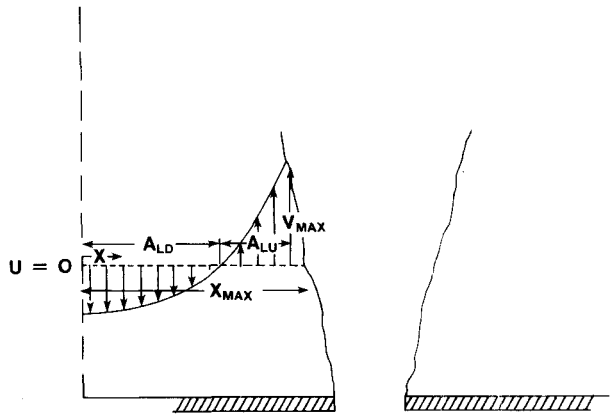

Figure A1. Model for zone of momentum transfer.

Appendix

Assume velocity profile (see Figure A1 for notation):

$$u = a + bx + cx^2$$

$$\left.\frac{du}{dx}\right|_{x=0} = b + 2cx = 0 \rightarrow b = 0$$

Therefore,

$$u = a + cx^2$$

Applying continuity,

$$\int_0^{x_{max}} u dx = 0 \rightarrow ax + \frac{cx^3}{3}\Big|_0^{x_{max}} = 0$$

Solving for a,

$$a = -\frac{cx_{max}^2}{3}$$

Substituting gives,

$$u = c\left[-\frac{x_{max}^2}{3} + x^2\right]$$

To determine A_{L_D}, find x where $u = 0$

$$x\Big|_{u=0} = \frac{x_{max}}{\sqrt{3}}$$

To determine $V_{max}/\overline{V}_L$

$$\overline{V}_L = \frac{1}{\left(\frac{x_{max}}{\sqrt{3}}\right)} \int_0^{\frac{x_{max}}{\sqrt{3}}} u dx = -\frac{2}{9} c x_{max}^2$$

However,

$$V_{max} = -\frac{cx_{max}^2}{3} + cx_{max}^2 = \frac{2}{3} cx_{max}^2$$

Therefore, the magnitude of V_{max} is three times that of $\overline{V}_L$.

Manuscript received Mar. 23, 1990, and revision received Feb. 11, 1991.